Parameter tuning of a MOSFET-based nerve membrane

Takashi Kohno* and Kazuyuki Aihara*†
* Aihara Complexity Modelling Project, ERATO, JST., Shibuya-ku, Tokyo, 151-0064
† Institute of Industrial Science, The University of Tokyo, Meguro-ku, Tokyo, 153-8505

Abstract

Two major principles for silicon neuron implementations are the phenomenological and the conductance-based ones. The former reproduces some properties perceived by the designers and does not claim mechanism consistency. The latter reproduces the dynamics of the ion channels on the nerve membranes. It makes the silicon neurons more similar to biological ones, but the implementations tend to be complicated because it attempts to replicate the detailed dynamics of the biological components. In the previous work [1], we proposed a new principle based upon phase plane analyses. It reproduces the mathematical structures of biological neurons, which makes the silicon neurons simple and faithful. In this paper, we show how Class 1 and Class 2 nerve membranes are realized by parameter tuning based on simple phase plane analyses with an illustrative MOSFET-based nerve membrane.

1 Introduction

Neural systems process massive and various incoming information flexibly, appropriately, and in real time. One of the purposes of studies on silicon neurons is to implement artificial systems that inherit these exquisite properties, and another is to produce some devices to interface between electrical circuits and living nerve systems [2]. There are two major types of silicon neuron design principles. One is the phenomenological implementation, which aims to reproduces some phenomena of biological neurons. Integrate-and-fire silicon neurons are good examples [3], which reproduce the integration property of spatio-temporal inputs and the threshold property of generating action potentials. Circuitries can be simple in these implementations but some properties that are not regarded may be lost. The other is the conductance-based implementation, which aims to reproduce some or all mechanisms in biological neurons faithfully. Most phenomena of biological neurons can be inherited in these implementations but circuitries tend to be complex. It is impossible to reproduce those mechanisms completely.

In the previous work [1][4], we proposed a design methodology that allows us to implement simple and biologically realistic silicon nerve membranes. It is based upon phase plane analyses that have been utilized to reveal the mathematical structures behind the properties of biological neurons. These properties can be given to simple silicon neurons by constructing the mathematical structures similar to that of biological neurons with silicon-friendly functions.

One of the well-known properties of biological neurons is oscillation against sustained input currents. Hodgkin [5] found in his biophysical experiments of stimulating various nerve membranes with sustained currents that some membranes start oscillating with an arbitrary low frequency when the currents exceed thresholds and others with non-zero frequency. He named the former Class 1 and the latter Class 2. Masuda and Aihara [6] indicated that these differences in excitation mechanisms may play a key role in neural coding. Bifurcation analysis studies on biological neuron models have revealed the mathematical structure behind the Class 1 and 2 excitabilities [7][8]. Typical bifurcations that lead to Class 1 excitability are a saddle-node on an invariant circle bifurcation and a saddle loop homoclinic orbit bifurcation. It is well known that Class 2 excitability can be produced by a Hopf bifurcation.

In this paper, we show how to tune the mathematical structure of silicon nerve membranes to make them reveal Class 1 or Class 2 excitabilities, utilizing a simple MOSFET-based nerve membrane as an example.

2 MOSFET-based nerve membrane

The design principle we proposed in the previous work [1] replicates the mathematical structures lying behind the properties of biological neurons with some 'MOSFET-friendly' functions. One of the simplest sil-

icon nerve membrane models based upon the generalized Hodgkin-Huxley equations can be described as follows:

$$C_y\frac{dy}{dt} = -\frac{y}{R_y} + \frac{\beta_m}{2}m^2 - \frac{\beta_n}{2}n^2 + a + I_{stim}, \quad (1)$$

$$\frac{dm}{dt} = \frac{f_m(y) - m}{T_m}, \quad (2)$$

$$\frac{dn}{dt} = \frac{f_n(y) - n}{T_n}, \quad (3)$$

where y represents membrane potential, m is a faster conductance variable, n is a slower conductance variable, C_y is membrane capacity, R_y is a constant resistance, a is a constant, I_{stim} is a stimulus current input, β_m and β_n are the transconductance coefficients of the MOSFETs for the ion channel current corresponding to m and n, respectively, and T_m and T_n are the time constants for m and n, respectively. Ordinarily we make T_m an order of magnitude smaller than T_n because the faster conductance corresponds to the sodium channel activation variable in the Hodgkin-Huxley equations and the slower one to the potassium channel activation variable. If we use the V-I characteristic curves of differential pairs (see appendix B for $x = m$ and n) as the sigmoidal functions $f_m(y)$ and $f_n(y)$, this system can be implemented with a very simple MOSFET circuitry [4].

Because the time scale for m is sufficiently smaller than that for n, we can reduce the faster conductance m by assuming it relaxes to $f_m(y)$ instantaneously. This reduction gives the slower subsystem that allows us to trace the system's behavior on the time scale of a whole generation of an action potential on a phase plane. The system equations are as follows:

$$C_y\frac{dy}{dt} = -\frac{y}{R_y} + \frac{\beta_m}{2}f_m^2(y) - \frac{\beta_n}{2}n^2 + a + I_{stim}, \quad (4)$$

$$\frac{dn}{dt} = \frac{f_n(y) - n}{T_n}. \quad (5)$$

Thus the y-nullcline and the n-nullcline are:

$$n = \sqrt{\frac{2}{\beta_n}(\frac{\beta_m}{2}f_m^2(y) - \frac{y}{R_y} + a + I_{stim})}, \quad (6)$$

$$n = f_n(y), \quad (7)$$

respectively. A typical relation between the two nullclines is shown in Fig. 1. The conditions that they have to satisfy for the system to inherit the fundamental properties of the biological neurons are discussed in [1].

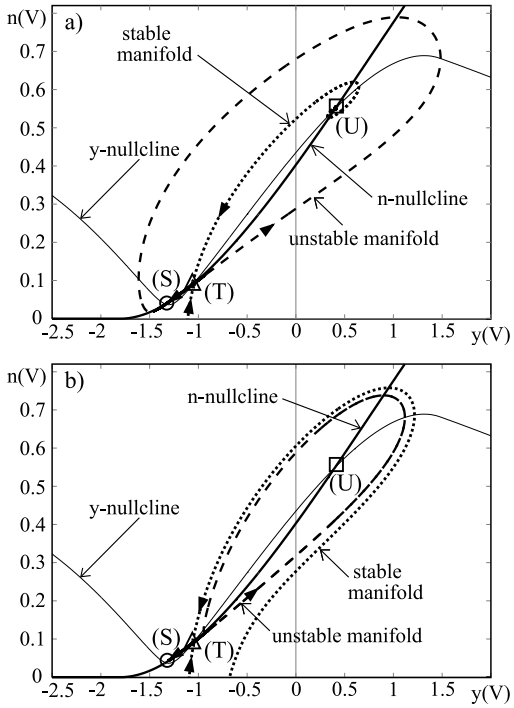

Figure 1: Typical phase planes of the slower subsystem. (S) is a stable equilibrium (the rest state). (T) is a saddle and (U) is an unstable equilibrium. a) The system is near a saddle-node on an invariant circle bifurcation. The parameters are shown in appendix A. b) The system is near a saddle loop homoclinic orbit bifurcation. The right segment of the unstable manifold of (T) wraps around a stable limit cycle around (U). The parameters are as in a) except C_y =0.0140(mF).

3 Parameter tuning for Class 1 and Class 2 excitabilities

3.1 Bifurcations of the rest state

The increase in the stimulus current transforms the phase space structure and destabilizes the rest state in our illustrative silicon nerve membrane like in most biological ones, which induces the repetitive firing. As described in the introduction, it is well known that Class 1 excitability is observed if the rest state loses stability via a saddle-node bifurcation or a saddle loop homoclinic orbit bifurcation, and the Class 2 excitability via a Hopf bifurcation [7][8]. These are the most major scenarios of repetitive firings. The phase plane structure near a saddle-node on an invariant circle bifurcation is shown in Fig. 1a). In this case, the stable

equilibrium point (S) and the saddle point (T) approach each other as the y-nullcline (eq. (6)) moves up in response to the increase in stimulus current I_{stim}. The smaller segment of the unstable manifold of (T) vanishes when (S) merges with (T), and the other segment of the unstable manifold turns to a stable limit cycle when they disappear. This limit cycle passes near the narrow channel between the y- and n-nullclines around the vanished saddle point, where the velocity is very slow. By narrowing this channel, we can delay the period of the limit cycle arbitrarily up to infinity when the channel width becomes zero. Figure 1b) shows the phase plane structure near a saddle loop homoclinic orbit bifurcation. In this case the right unstable manifold of (T) gets closer to the upper stable manifold as the y-nullcline moves up, until it merges with the upper segment of the stable manifold and becomes a closed homoclinic orbit. Then a stable limit cycle is born around (U), which passes near the saddle point where the velocity is very slow. In contrast to above two scenarios, the saddle point (T) has no role in the Hopf bifurcation. The rest state loses stability singularly, and the system moves to a stable limit cycle around it if one exists. Because the system jumps to a limit cycle, the repetitive firing begins abruptly with a certain non-zero frequency.

3.2 Tuning the bifurcations

As described in the above subsection, the stability of the rest state plays a key role in neural excitabilities. The local linearization method tells how it depends on the parameters. The necessary and sufficient conditions for an equilibrium point to be stable are:

$$\lambda_1 + \lambda_2 < 0 \Leftrightarrow \eta'(y_0) < \frac{C_y}{n_0 \beta_n T_n}, \tag{8}$$

$$\lambda_1 \cdot \lambda_2 > 0 \Leftrightarrow \eta'(y_0) < f_n'(y_0), \tag{9}$$

where λ_1 and λ_2 are the eigenvalues of the Jacobian matrix in equations (4)-(5), (n_0, y_0) denotes an equilibrium point, $'$ denotes $\frac{d}{dy}$, and $\eta(y)$ is the right side of eq. (6). These conditions indicate that at a stable equilibrium point the y-nullcline should cross the n-nullcline from over to under and the gradient of the y-nullcline should keep smaller than a certain value. Thus the stabilities of the equilibrium points can be configured as in Fig. 1 if we place the leftmost cross-point of the y-nullcline and the n-nullcline where the gradient of the y-nullcline is sufficiently small and the rightmost one where it is sufficiently large. Of course we must tune C_y and T_n properly so that $\frac{C_y}{n_0 \beta_n T_n}$ is between these two gradients. In this situation, (S) and (T) get closer as the y-nullcline moves up and (S) loses stability when they merge because condition (9) is no longer satisfied. This is the common scenario for Class 1 excitability. If the rightmost side of condition (8) is smaller than $f_n'(y)$ at the point where (S) and (T) merge, (S) loses stability singularly via the Hopf bifurcation before merging with (T). This is the basic scenario for Class 2 excitability. To obtain a Class 2 nerve membrane that generates action potentials of a reasonable size and keeps firing repetitively for a reasonably wide range of stimulus current, the y-nullcline should be shifted right to make (T) and (U) disappear or, at least, to make (S) and (T) further aprat than in Fig. 1. Class 2 excitability in our silicon nerve membrane is discussed in [1].

The local stability analysis does not tell which of the two scenarios appears. The bifurcation diagrams for these scenarios are shown in Fig. 2. Let us trace

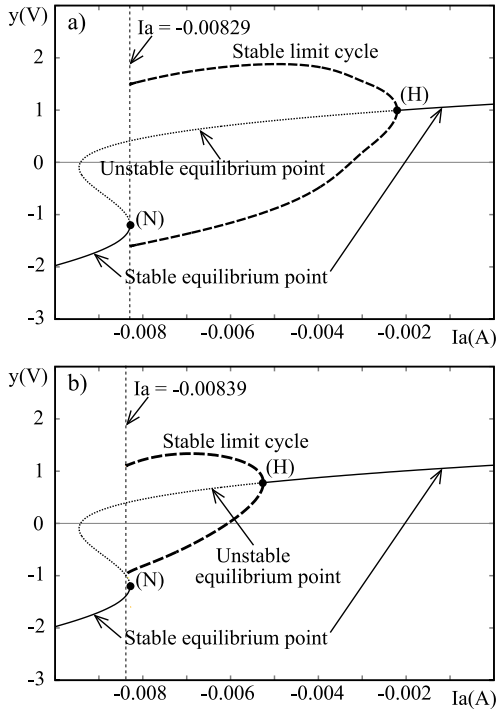

Figure 2: The bifurcation diagrams for a) a saddle-node on invariant circle bifurcation and b) a saddle loop homoclinic orbit bifurcation. (N) represents the point where the stable and saddle points merge and (H) the point where the stable limit cycle emerges. a) The limit cycle vanishes at I_a =-0.00829(A) where (N) exists. The parameters are as in Fig. 1 a) except I_a is swept. b) The limit cycle vanishes at I_a =-0.00839(A). The parameters are as in Fig. 1 b) except I_a is swept.

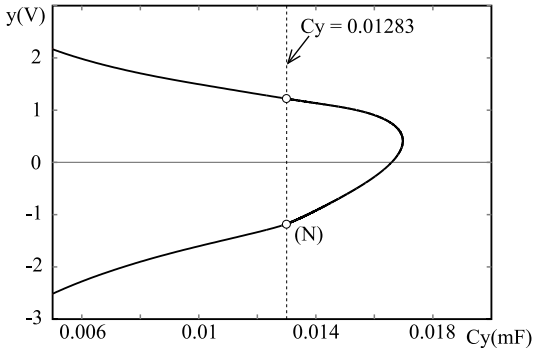

Figure 3: The bifurcation diagram of the limit cycle along C_y. Parameters are as in appendix A except $I_a = -0.00829$(A) and C_y is swept. The vertical axis represents the upper and lower limits of the limit cycle. The white circles at C_y =0.01283(mF) represent the limit cycle is unstable around it.

them from right to left. In both cases, the limit cycle that emerges via the Hopf bifurcation continues with its amplitude increasing. If the amplitude is sufficiently large at the point where the pair of stable and saddle points emerges ((N) in Fig. 2, where I_a = -0.00829(A)), the orbit of the limit cycle gets 'trapped' and vanishes; otherwise it persists until it merges with the unstable manifold of the saddle point.

The amplitude of the limit cycle can be controlled by C_y, which works as a time scale factor. It gets smaller as C_y becomes larger because the velocity of the system in the y direction decreases. In Fig. 3, we show the bifurcation diagram of the limit cycle for an I_a value just near the point (N) in Fig. 2. The limit cycle is stable except when the limit cycle passes at the point (N) ($C_y \simeq 0.01283$(mF) in Fig. 3). Thus, we obtain the saddle-node on invariant circle bifurcation if C_y is below 0.01283 (mF) and the other one if it is above.

4 Conclusions

We have shown how Class 1 and Class 2 excitabilities are obtained with a MOSFET-based nerve membrane. Once the phase plane structure is configured properly by tuning the parameters that affect the forms of the nullclines, we can easily realize the desired neural excitability by tuning C_y and T_n. We have shown that the two types of Class 1 excitabilities can be selected only by tuning C_y. Because the ratio of the time scales of y and n affects the amplitude of the limit cycle, T_n can also be tuned. This paper indicates that our illustrative MOSFET-based nerve membrane can function as a Class 1 or Class 2 nerve membrane according to the proposed parameter tuning.

References

[1] T. Kohno and K. Aihara, "Design of Neuromorphic Hardware Based upon Mathematical Methods," *Proc. SBRN 2004*, 3470, 2004.

[2] M. Simoni, G. Cymbalyuk, M. Sorensen, et al., "A Multiconductance Silicon Neuron With Biologically Matched Dynamics," *IEEE Trans. Biomed. Eng.*, Vol. 51, No. 2, pp. 342-354, Feb., 2004.

[3] D. Rubin, E. Chicca, and G. Indiveri, "Characterizing the firing properties of an adaptive analog VLSI neuron," *Proc. Bio-ADIT 2004, Lausanne*, pp. 314-327, 2004.

[4] Takashi Kohno and Kazuyuki Aihara, "A MOSFET-based model of a Class 2 Nerve membrane," *Submitted to IEEE Trans. Neural Networks.*

[5] A. L. Hodgkin, "The local electric changes associated with repetitive action in a non-medullated axon," *J. Physiol.*, Vol. 107, pp. 165-181, 1948.

[6] Naoki Masuda and Kazuyuki Aihara, "Band-pass filtering properties of interspike interval encoding with Morris-Lecar neurons," *Proc. SBRN 2004*, 3611, 2004.

[7] J. Rinzel and B. Ermentrout, *"Analysis of Neural Excitability and Oscillations," in "Methods in Neural Modeling", ed. C. Koch and I. Segev*, pp. 251-291, MIT Press, 1998.

[8] E. M. Izhikevich, "Neural Excitability, Spiking, and Bursting," *International Journal of Bifurcation and Chaos*, Vol. 10, pp. 1171-1266, 2000.

Appendix

A Parameters:

Parameter	Value	Parameter	Value
β_m	0.0406 (A/V^2)	β_n	0.0799 (A/V^2)
δ_m	-0.5200 (V)	δ_n	0.8000 (V)
ϵ_m	2.000 (V)	ϵ_n	2.600 (V)
$\bar{m}$	1.300 (V)	$\bar{n}$	1.400 (V)
T_m	0.1300 (ms)	T_n	1.500 (ms)
C_y	0.0100 (mF)	R_y	200 (Ω)
a	0 (A)	I_A	-0.00834 (A)

B Characteristics of differential pairs:

$$f_x(y) \equiv \begin{cases} \bar{x} & when \quad y > \delta_x + \epsilon_x, \\ \frac{\bar{x}}{2}\{1 + \frac{1}{\epsilon_x^2}(y-\delta_x)\sqrt{2\epsilon_x^2 - (y-\delta_x)^2}\} & \\ & when \quad \delta_x - \epsilon_x \le y \le \delta_x + \epsilon_x, \\ 0 & when \quad y < \delta_x - \epsilon_x, \end{cases}$$